A FEASIBILITY STUDY OF AN ATOMIC RATE GYRO

DAVID SEAGRAVE TWINING

UNITED STATES
NAVAL POSTGRADUATE SCHOOL

THESIS

A FEASIBILITY STUDY OF
AN ATOMIC RATE GYRO

by

David Seagrave Twining

Captain, United States Marine Corps

1969

A FEASIBILITY STUDY OF
AN ATOMIC RATE GYRO

* * * * *

David Seagrave Twining

A FEASIBILITY STUDY OF
AN ATOMIC RATE GYRO

by

David Seagrave Twining

Captain, United States Marine Corps

Submitted in partial fulfillment of
the requirements for the degree of

MASTER OF SCIENCE
IN
ENGINEERING ELECTRONICS

United States Naval Postgraduate School
Monterey, California

1 9 6 0

A FEASIBILITY STUDY OF AN ATOMIC RATE GYRO

by

David Seagrave Twining

This work is accepted as fulfilling
the thesis requirements for the degree of
MASTER OF SCIENCE
IN
ENGINEERING ELECTRONICS
from the
United States Naval Postgraduate School

ABSTRACT

The purpose of this paper is to describe the investigation of the feasibility of utilizing the precessional motion of atoms to measure the rotation of a given reference frame. During this investigation, experiments were made which led to the construction of a system which was able to detect rotation by measuring such a precession. The system used rubidium 87, the atoms of which, in a magnetic field, precess in a direction dependent upon the quantum state of the atom.

The theoretical investigation and system development were performed at the instrument division of Varian Associates in Palo Alto, California, during the period January to March, 1960, while the writer was a student in the Engineering Electronics curriculum at the U. S. Naval Postgraduate School, Monterey, California.

The writer wishes to thank William E. Bell and Dr. Arnold L. Bloom of Varian Associates for their assistance and suggestions. In conclusion, thanks are expressed particularly to Professor Carl E. Menneken of the U. S. Naval Postgraduate School for his encouragement and criticisms in the preparation of this paper.

TABLE OF CONTENTS

LIST OF ILLUSTRATIONS

I. Introduction.

The advent of the long range guided missile and the space vehicle has imposed an ever increasing burden on the components of inertial guidance systems. Accelerometers, free gyroscopes, and rate gyroscopes are subject to the very large forces of powered flight, and yet must perform within minute tolerances for increasingly protracted periods. The mechanical nature of these instruments aggravates the problem. In the case of the gyroscope, infinitesimal inaccuracies in bearing or gimbal may cause torques which produce unwanted precessions. The cumulative effect of such precessions is to produce unacceptable errors.

The performance of gyroscopes has been improved considerably by the use of advanced gimbal systems, and it is probable that much additional progress can yet be made. Nevertheless, all such systems are inherently susceptible to the stresses imposed upon them by a harsh mechanical environment.

A solution to the problem of the rate gyroscope is suggested by the precession of atomic spin systems. Such a solution would have the advantages of greater inherent accuracy, mechanical simplicity, and physical durability.

A system capable of measuring such precessions, and employing optical pumping in alkali vapor was suggested to the writer by Dr. Martin Packard and Dr. Arnold Bloom of Varian Associates in Palo Alto, California. The alkali metal chosen was rubidium 87 because of its convenient hyperfine spectrum.

This thesis describes the theory and the experimental work

performed at Varian Associates by the writer to demonstrate the feasibility of such an "atomic rate gyroscope".

II. Theoretical Background

A. Energy Levels

The Rubidium Atom

Rubidium, the 37th element, is an alkali metal in the same group as are lithium, sodium, potassium, cesium, and francium. These elements have been studied extensively because of the simplicity of their optical spectra. The structure of the spectral lines of the alkali metals is quite similar, and results from the basic atomic characteristic of the group. This character stic is that there is a single valence electron outside of the closed electron shells which contain the remaining electrons. This single valence electron allows a quantum mechanical description which is relatively less complicated than in the case of other atoms.

There are two naturally occurring isotopes of rubidium. Rubidium 85 has a relative abundance of 72.8% and rubidium 87 has a relative abundance of 27.2%. Because of a difference in the hyperfine spectrum, rubidium 87 is easier to use in demonstrating the effect of rotation.

An atom with a single valence electron will be found, on the average, to occupy the lowest possible energy state with the valence electron in an S state. In the case of rubidium, this is the 5S state. The number 5 is the quantum number designated n, and in the one electron atom completely determines the energy. Because of the shielding effect of the electrons in the closed shells, however, other factors contribute to the energy of the rubidium atom.

An atom in an S state has zero angular momentum, if the spins of the electron and the nucleus are neglected. Angular momentum is designated by the quantum number L; in this case, L=0. The energy of the atom is partially determined by its angular momentum. Thus, the L=1 state designates a higher energy level than does L=0. The n=5,L=1 state is denoted 5P. There are many higher energy levels to which the atom can be excited, but these are not utilized in the optical pumping to be described.

The transition from a 5P state to a 5S state causes the emission of the characteristic light of rubidium, a deep red at the edge of the visible spectrum.

The Fine Structure

Up to this point, the spin of the electron has been neglected. As the spin contributes to the total angular momentum, it must be included. The spin state of an electron is designated by the quantum number s, and may be either +1/2 or -1/2. The total angular momentum is now designated by the quantum number j, which is the absolute value of the sum of s and L. Thus in an S state, where L=0, j must equal 1/2. In a P state, however, j can be either $|1+1/2| = 3/2$ or $|1-1/2| = 1/2$. Thus it is seen that the P state is split into two levels. These are denoted $P_{1/2}$ and $P_{3/2}$ and have slightly different energies. Transitions occurring between these P levels and the S level result in two spectral lines close together at 7948 Å and at 7800 Å as shown in Fig. 2.1. These two lines are an example of fine structure, and form a spectral doublet. They may be separated easily with an optical interference filter.

The Hyperfine Structure

As optical resolution techniques improved, it became evident that within the fine structure there was additional or hyperfine structure. It was discovered that this was caused by the effect of the angular momentum of the nucleus itself. Nucleons, like electrons, have a spin; and the spin of the nucleus is the resultant of the spin of its nucleons. This spin is designated by the quantum number I, and may range from zero, in the case of nuclei containing an even number of protons and an even number of neutrons, to as much as seven for lutecium 176[1]. For rubidium 87, I is equal to 3/2.

It must be noted that the quantum number n has the greatest effect on the energy, while the quantum number L is of secondary importance. The effect of s is relatively minor, and the effect of I is so slight as to influence the energy of the atom by an almost insignificant amount. The effect of I upon the structure of the energy levels, however, is of great importance.

A new quantum number, F, can now be defined. This is the resultant of j and I. The addition is accomplished vectorially with the conditions that F be integral or half integral, and that possible values of F be separated by integers. Thus, for $j=3/2$ and $I=3/2$, F may be 3, 2, 1, and 0. This is shown graphically in Fig. 2.2a. For $j=1/2$ and $I=3/2$ there are only two possibilities, $F=2$ and $F=1$. These are shown in Fig. 2.2b. It is seen that the two P states now have six levels, four for $P_{3/2}$

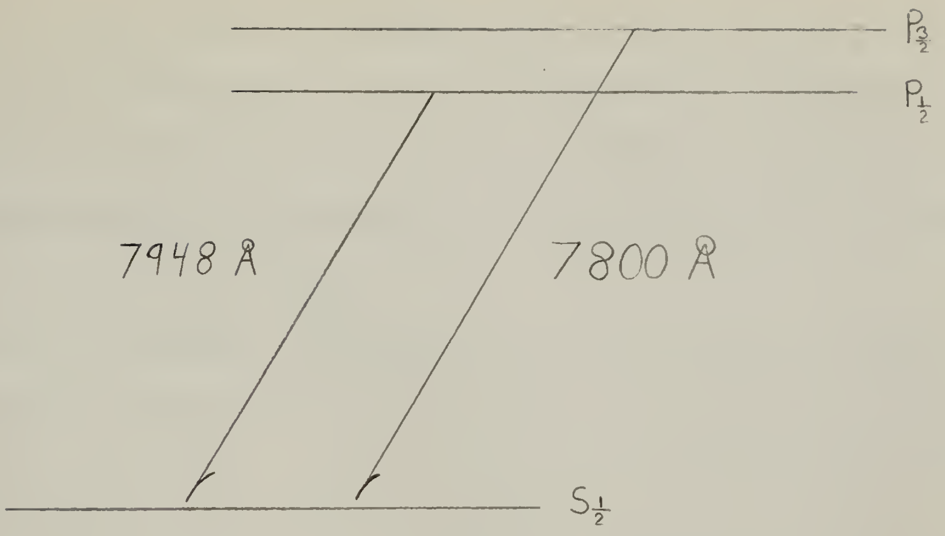

Fig. 2.1

Fine Structure Energy Level Diagram

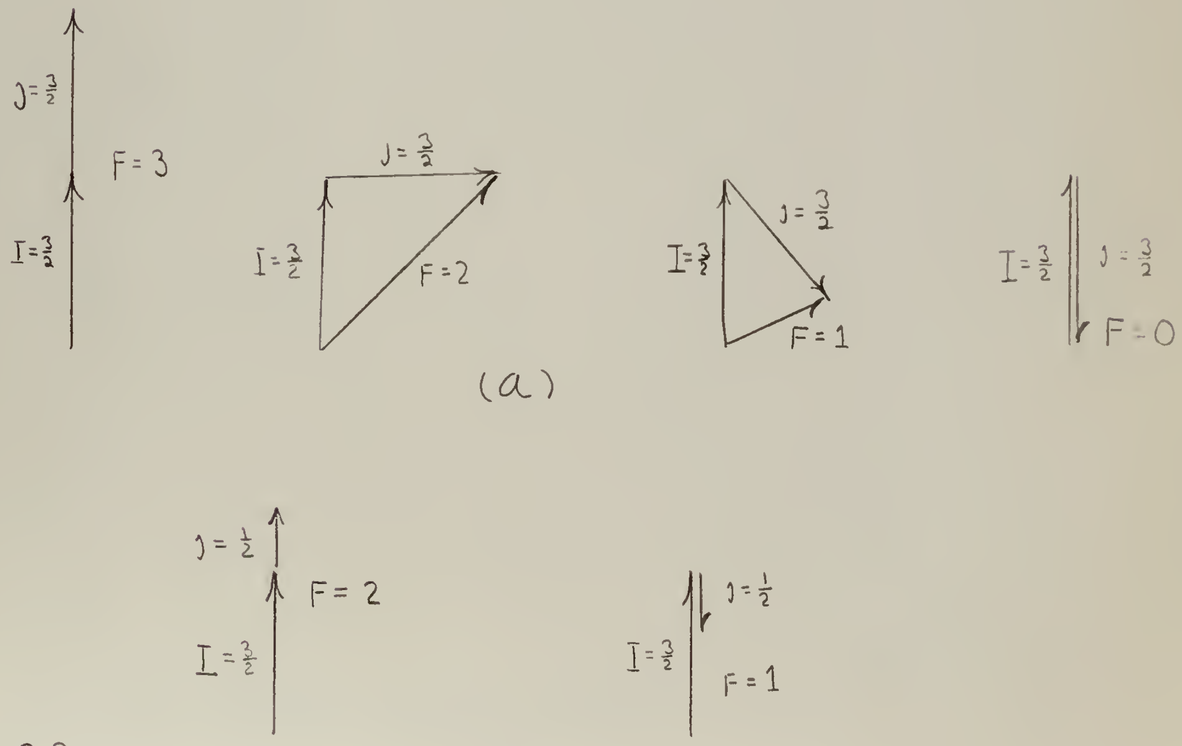

(a)

(b)

Fig 2.2

Vector Diagram of j and I Addition

and two for $P_{1/2}$, while the S state is split into two levels. The energy level diagram shown in Fig. 2.3 exaggerates the separations of the hyperfine levels in comparison with the fine splitting, and likewise exaggerates the fine splitting in comparison with the separation between the S and the P states.

There are a number of transitions which may take place between these energy levels subject to the selection rules of quantum mechanics which are, $\Delta L \overset{0}{=} \pm 1$, $\Delta j = 0, \pm 1$, and $\Delta F = 0, \pm 1$. From these selection rules, and from the energy level diagram, the actually observed spectrum can be predicted.

1. G.E. Pake NMR Solid State Physics Vol. 11

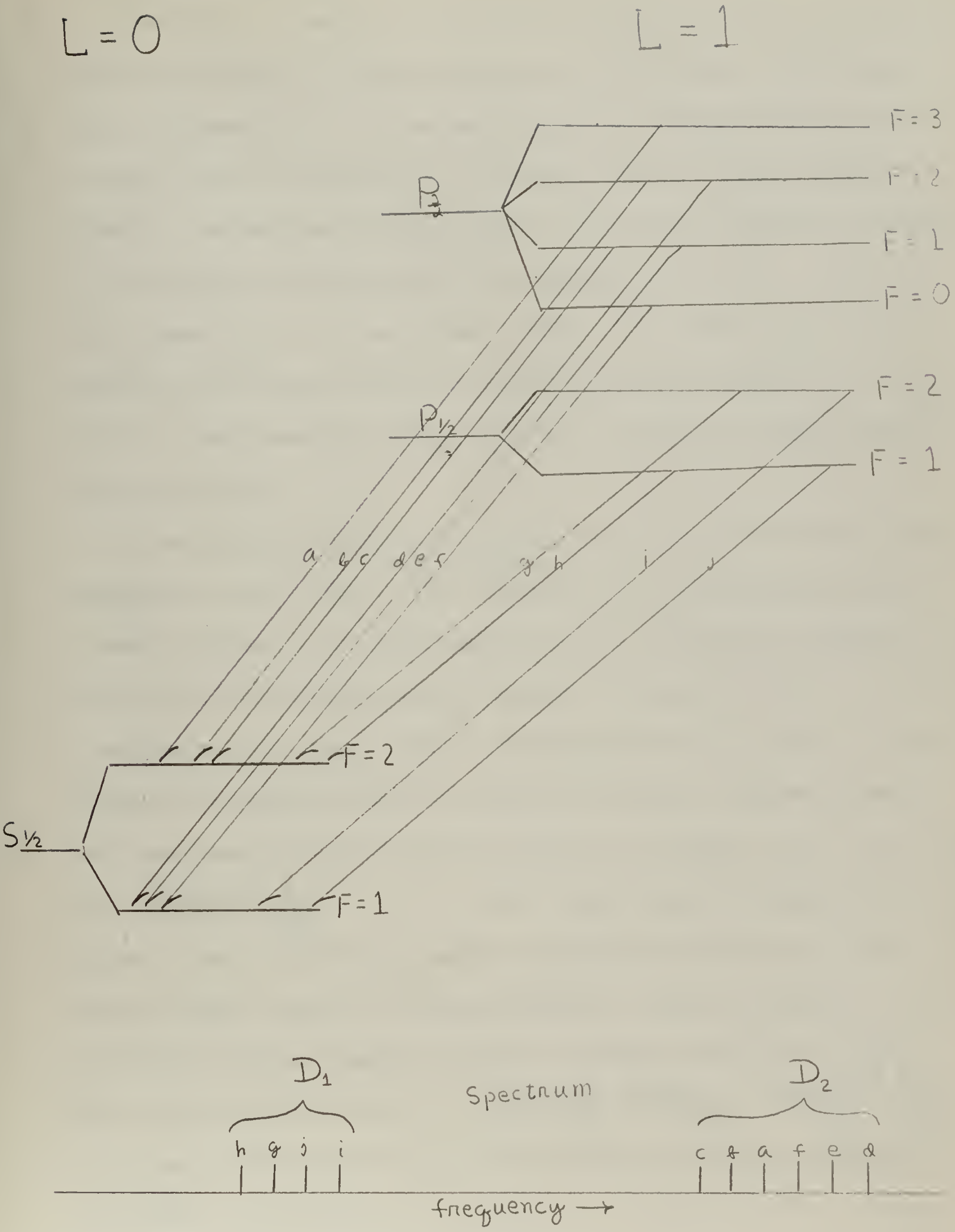

Fig. 2.3 Energy Level Diagram Showing Hyperfine Spectrum

The Zeeman Splitting

Additional complexity is introduced when the effect of a magnetic field is included, for the orientation of the atomic spin systems with reference to an external magnetic field determines additional energy terms to be added to the existing levels. These additional energy terms separate a given level into discrete sublevels according to the discrete orientations of the atomic spin systems. These sublevels are referred to as Zeeman levels. The relationship of spin orientation to energy exists because the spinning charges of an atom produce local magnetic fields which have alignment energies with the external field.

The angular momentum and magnetic moment of an atom will now be examined in more detail. The solutions to the Schrödinger equation contain the various quantum numbers, and wave mechanics determines the conditions under which they may appear. It has been seen that j is a combination of L and s, while F is a combination of j and I. These numbers are representations of angular momentum. Quantum mechanics dictates that the actual angular momentum associated with F, for example, is $\sqrt{F(F+1)}\,\frac{h}{2\pi}$. This total angular momentum has no fixed vector direction as might be expected from classical theory. It does, however, possess a maximum projected component along a reference direction, say the magnetic field of the earth, which is $F\frac{h}{2\pi}$. The other possible components are $(F-1)\frac{h}{2\pi}, (F-2)\frac{h}{2\pi}, \ldots (-F+1)\frac{h}{2\pi}, -F\frac{h}{2\pi}$. These projected components are denoted by another quantum number, M, such that $-F \leqq M \leqq F$.

When it is considered that the total angular momentum of the atom, $\sqrt{F(F+1)}\frac{h}{2\pi}$ is the vector sum of $\sqrt{j(j+1)}\frac{h}{2\pi}$ and $\sqrt{I(I+1)}\frac{h}{2\pi}$ and that also $F = |j \pm I|$ it is apparent that there must be an angle between $\bar{j}$ and $\bar{I}$. In the ground state of rubidium 87 where j= 1/2 and I= 3/2, F must equal either 1 or 2. $|\bar{F}|$, however, is $\sqrt{2}$ or $\sqrt{6}$, while $|\bar{j}| = \frac{1}{2}\sqrt{3}$ and $|\bar{I}| = \frac{1}{2}\sqrt{15}$. The vector addition diagrams for F = 1 and F = 2 are shown in Fig. 2.4.

Next, the relationship of the magnetic moments to these angular momenta will be investigated. The magnetic moment, $\bar{\mu}_L$, associated with a given value of L is given by wave mechanics to be $\bar{\mu}_L = \frac{-e}{2mc}\bar{G}_L$ where $\bar{G}_L$ is the angular momentum due to the orbital motion of the electron. Similarly, $\bar{\mu}_s = -\frac{e}{mc}\bar{G}_s$ is the magnetic moment due to electron spin. The total electronic magnetic moment is then $\bar{\mu}_j = -\frac{e}{2mc}(\bar{G}_L + 2\bar{G}_s)$. It should be noted that the magnetic moment vector is directed oppositely from the angular momentum vector. The nucleus also has a magnetic moment but it is less than one percent of the electronic magnetic moment, and, in the case of rubidium 87, directed along the nuclear spin vector.

The result of this is an important qualitative difference between the F=1 and the F=2 states. If the magnetic moment vectors are added to the vector diagrams used to illustrate the addition of j and I, it is seen in Fig. 2.5a that for the F=2 state the projection of $\bar{\mu}_F$ on $\bar{F}$ is in the opposite direction from $\bar{F}$. Conversely, in Fig. 2.5b it is shown that for the F=1 state the projection of $\bar{\mu}_F$ is in the same direction as $\bar{F}$. Also it should be noted that μ_F is slightly greater in the F=1 state.

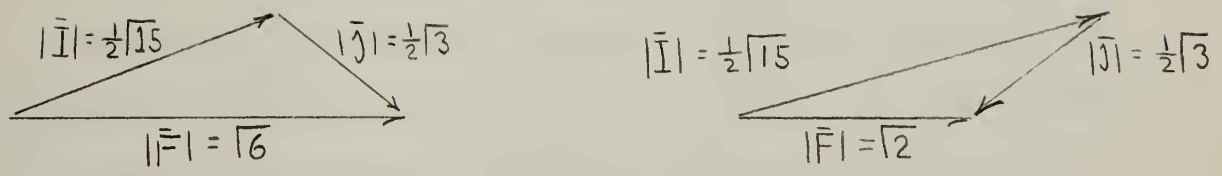

Fig 2.4 Angular Momentum Vector Diagram

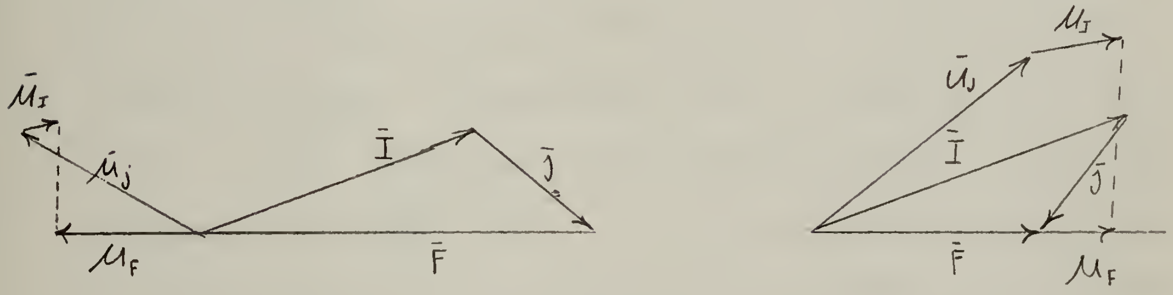

Fig. 2.5 Magnetic Moment Vector Diagram

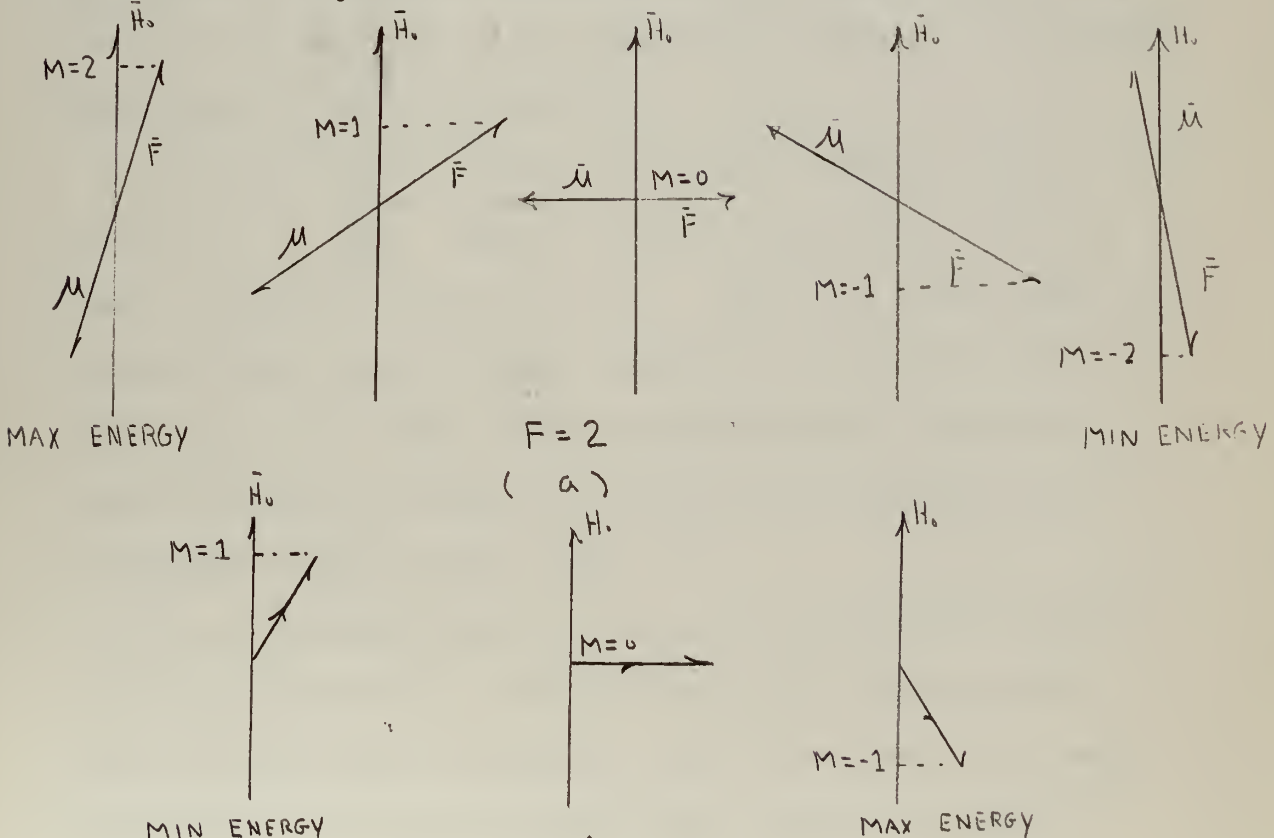

F = 2

(a)

F = 1 (b)

Fig 2.6 Diagram of Energy Relation to M

When the rubidium atom is in a magnetic field the F=1 and the F=2 levels are split into the various Zeeman sublevels. First consider the F=2 level. As indicated previously, the angular momentum vector, $\bar{F}$, may have certain projections on the external field vector. These projections, designated M, indicate the angular momentum in the direction of the external field. Thus the angular momentum component, G_{H_o}, equals $\frac{M\,h}{2\,\pi}$ where M=2, 1, 0, -1, -2. For the F=1 state M can be 1, 0, -1. When an external field exists, these M levels have different energies. The additional energy is caused by the orientation of $\bar{\mu}_F$ with respect to the external field H_o. This energy is given by $W_H = -\bar{\mu}_F \cdot \bar{H}_o$. It is seen that for M=2, $\bar{\mu}_F$ is directed away from $\bar{H}_o$ and W_H is maximum positive. When M equals -2, $\bar{\mu}_F$ is directed towards $\bar{H}_o$ and W_H is maximum negative. Thus, in this case, for the five Zeeman split sublevels, the highest energy level is that for which M=2.

For the F=1 level, however, a different situation exists. For M=1, the $\bar{\mu}_F$ vector is almost in line with H_o, and the energy is minimum, while for M= -1, $\bar{\mu}_F$ is almost oppositely directed from H_o and the energy is maximum. This is shown graphically in Fig. 2.6. There is now enough information available to construct a complete energy level diagram for the ground state of rubidium 87. This is shown in Fig. 2.7.

There are several points to note in this energy level diagram. The distance between the individual Zeeman split components is greatly exaggerated for a magnetic field such as that of the earth. The distance between the F=1 Zeeman split components slightly

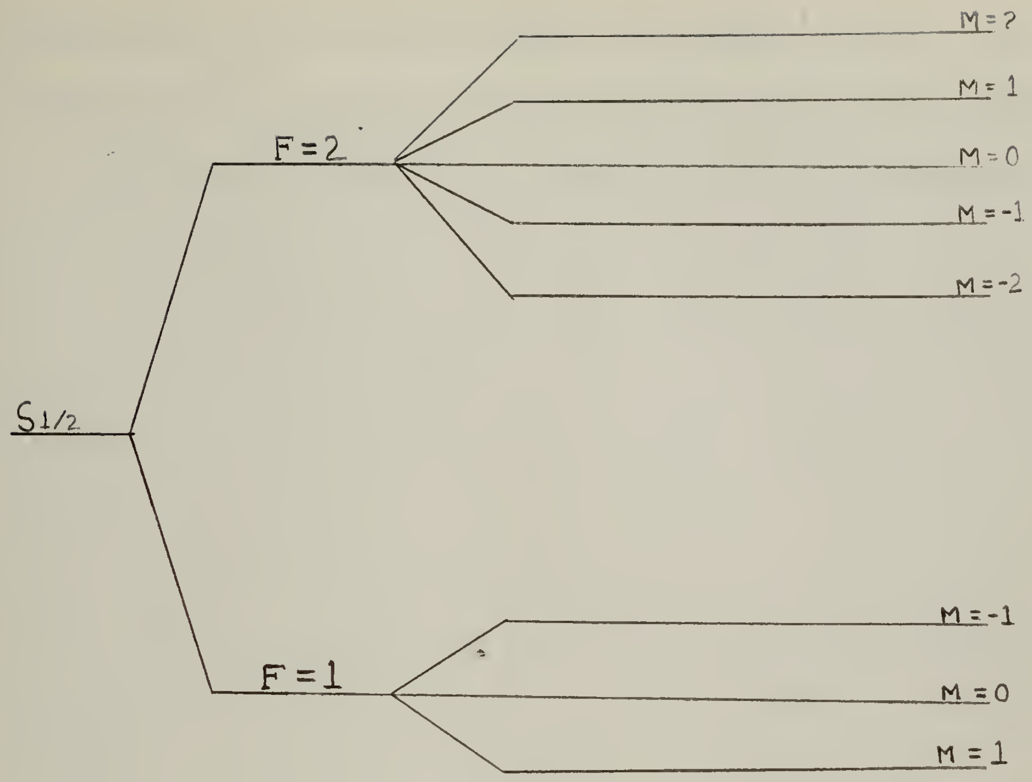

Fig. 2.7 Zeeman Split Ground State Energy Level Diagram

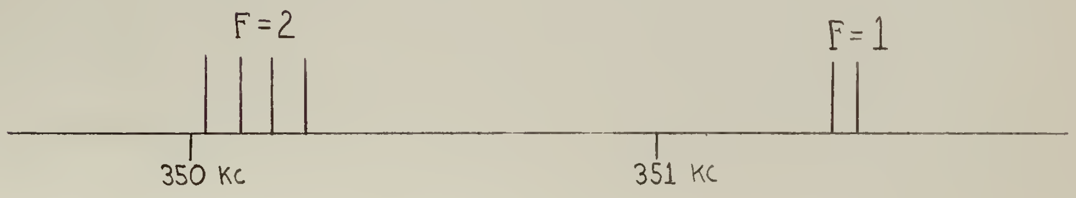

Fig 2.8 Zeeman Spectrum Diagram

exceeds that of the F=2 group because the magnetic moment, $\bar{\mu}_F$ is slightly greater in the F=1 case as described previously. Finally, the inversion of the M sublevels should be noted in the F=1 group.

The Transitions

As a consequence of the above energy level diagrams, there are several types of transitions which may occur. The first, which has already been discussed, is an optical transition with "D" lines at 7800 Å and 7948 Å. It is seen that these lines will be hyperfine split, but the relative energy difference is so small that the effect will be extremely difficult to observe without the use of very large magnetic fields.

There are also transitions between the levels in the ground state. These are forbidden in the normal sense, because $\Delta L = 0$, but may be stimulated and have a certain probability of occurring spontaneously.

The transitions from the F=2 group to the F=1 group occur when stimulated by radio frequency quanta which have the same energy as the level separation. For the M=0, F=2 to the M=0, F=1 transition, the field independent transition, this frequency is 6834 Mc. In the near vicinity of this line there will be others somewhat dependent upon the magnetic field. The transitions occurring will be those for which $\Delta M=0$ or ± 1.

There will also be transitions occurring within the F=2 group and within the F=1 group. The frequencies here vary directly with the magnetic field. In the field of the earth in the vicinity of Palo Alto, California, the approximate transition frequency is 350 Kc. Even within the F=2 group and the F=1 group the levels are not precisely equidistant, but the difference amounts to only a few cycles per second. The sublevels in the F=1 group have slightly

wider separations than do the sublevels in the F=2 group. As a consequence, the F=1 transitions have a frequency approximately 1000 cycles per second higher than do the F=2 transitions. Fig. 2.8 shows the approximate spectrum. It is with this spectrum that the remainder of this thesis shall be most concerned.

B. The Pumping Action

The Process

The energy difference between the various Zeeman split levels is slight, and is far exceeded by k T, where k is Boltzman's constant and T is the temperature in degrees Kelvin. For this reason it might be expected that the energy levels are rather evenly populated. To observe transitions, there must first occur an imbalance in population. Then, the return to the normal population will produce an observable effect. There must exist some method for creating such an abnormal population distribution, and this process is termed "pumping".

The optical pumping method will now be described. The sample, in this case rubidium vapor, is irradiated with one of the "D" lines of the rubidium spectrum, usually the D_1 line. Photons of this light excite the rubidium atoms out of the ground state into the $P_{1/2}$ state. This is done in such a manner that more atoms are excited from the lower sublevels of the $F=2$ and $F=1$ states than from the higher levels. The excited atoms immediately return to the ground state by the emission of a photon, arriving randomly. In this manner, the lower levels are depleted while the upper levels are over-populated.

Population Probabilities

The pumping light is emitted from a rubidium spectral lamp with both D lines present. An interference filter removes the D_2 line. Next the light is passed through a circular polarizer. The result is that the photons which pass through carry with them an angular momentum, and any atom which absorbs such a photon must change its angular momentum such that $\Delta M = +1$.

It is easily seen that this condition cannot be met in the $M = +2$ case, for the highest $P_{1/2}$ substate is $M = +2$. Thus, the probability of an atom being excited out of the $M = +2$ substate is zero. The remaining relative transition probabilities can be calculated by an application of the matrix elements for electric dipole excitation ($\Delta M = +1$)[1]. This calculation has been carried through for rubidium 87 by Dehmelt, and the following probabilities obtained:

$$(P_{-1}: P_0: P_{+1}):(P_{-2}:P_{-1}:P_0:P_{+1}:P_{+2}) =$$
$$\left[(1+5R): (2+4R): (3+3R)\right] : \left[(4+2R): (3+3R): (2+4R): (1+5R):(6R)\right]$$

In this formula, R is the ratio of the intensity of the D_2 light to that of the D_1 light. With the interference filter, R becomes zero and the probabilities become $[1:2:3] : [4:3:2:1:0]$.

The rubidium vapor is enclosed in a pyrex container holding an inert buffer gas at a pressure of 3 Cm Hg. This buffer gas has two functions. First, it reduces collisions of rubidium atoms with the

---

1. E. U. Condon and G. H. Shortley, Theory of Atomic Spectra (Cambridge University press, New York, N Y. 1935)

wall of the gas cell. Wall collisions tend to make atoms in the S state lose their orientation, while collisions with atoms of the buffer gas have no such effect. Second, the atoms in the P state, because of their different wave function, are completely reoriented by buffer gas collisions even though the time spent in the P state is very short.

Thus the return to the S state is random. The result is a population distribution such that if A_m represents the relative saturation population of the m^{th} substate, then

$$(A_{-1}:A_0:A_1):(A_{-2}:A_{-1}:A_0:A_1:A_2) = (P_{-1}^{-1}:P_0^{-1}:P_1^{-1}):(P_{-2}^{-1}:P_{-1}^{-1}:P_0^{-1}:P_1^{-1}:P_2^{-1})$$

It is apparent that if it were not for various relaxation effects, only the F=2, M=2 sublevel would be populated. Because of relaxation, residual D_2 light, and imperfect polarization, the pumping is never complete. Nevertheless, there is a strong tendency for the upper levels of the F=2 group to be over populated and, to a lesser degree, a tendency for the upper level of the F=1 group to be over populated.

C. The Larmor Precession

The rubidium atom has been shown to be a small magnet with angular momentum. It should be expected, therefore, that the atom will precess when placed in an external magnetic field such as that of the earth. Such a precession is actually observed, and the rate of precession, ω, may be calculated both by classical methods and by means of quantum mechanics with equal success. The precession problem will here be examined from a classical viewpoint.

Assume a magnetic field along the z axis, and a magnetic moment aligned with an angular momentum at some angle to the z axis (see Fig. 2.9). It follows from elementary electromagnetic field theory that a torque $\bar{L}$ is produced such that $\bar{L} = \bar{\mu}_M \times \bar{H}_0$. Then, from mechanics, $\frac{d\bar{M}}{dt} = \bar{L} = \bar{\mu}_M \times \bar{H}_0$. To show directly that a precession, ω, ensues is rather lengthy[1]. Instead, proceeding indirectly, postulate a second coordinate system which rotates about the z axis with a frequency, ω. Now the change in angular momentum, as viewed from the second system, due only to the rotation of the system, is $-\bar{\omega} \times \bar{M}$, and thus the total change in angular momentum, as viewed from the second system, $\left(\frac{d\bar{M}}{dt}\right)^*$, is

$$\left(\frac{d\bar{M}}{dt}\right)^* = \frac{d\bar{M}}{dt} - \bar{\omega} \times \bar{M} = \bar{\mu} \times \bar{H}_0 - \bar{\omega} \times \bar{M}$$

---

[1] G. E. Pake
Solid State Physics, Vol. 11, Academic Press Inc., Publishers
New York 10, N. Y. 1956

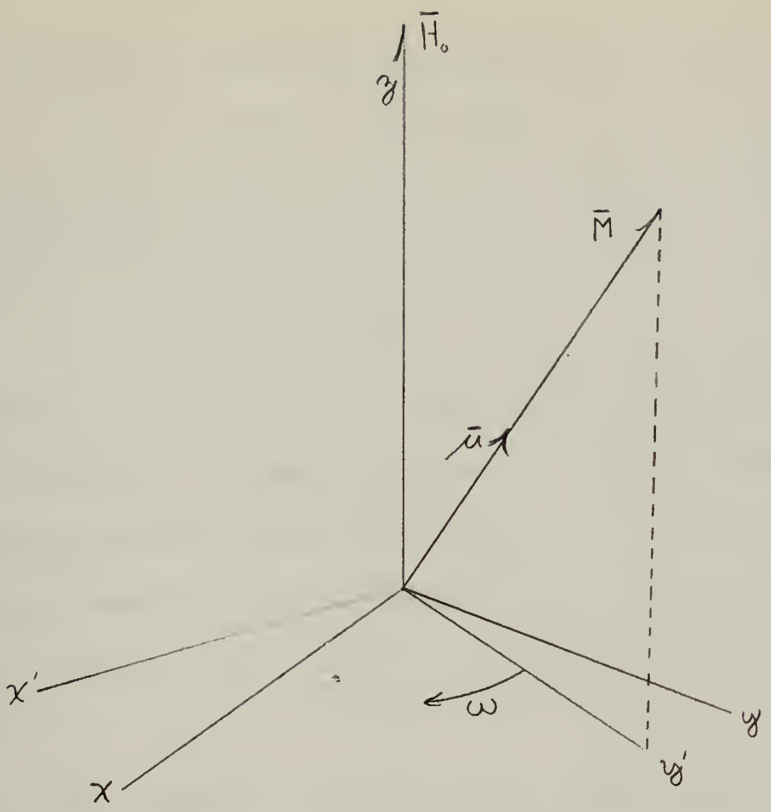

Fig. 2.9 Precession Vector Diagram

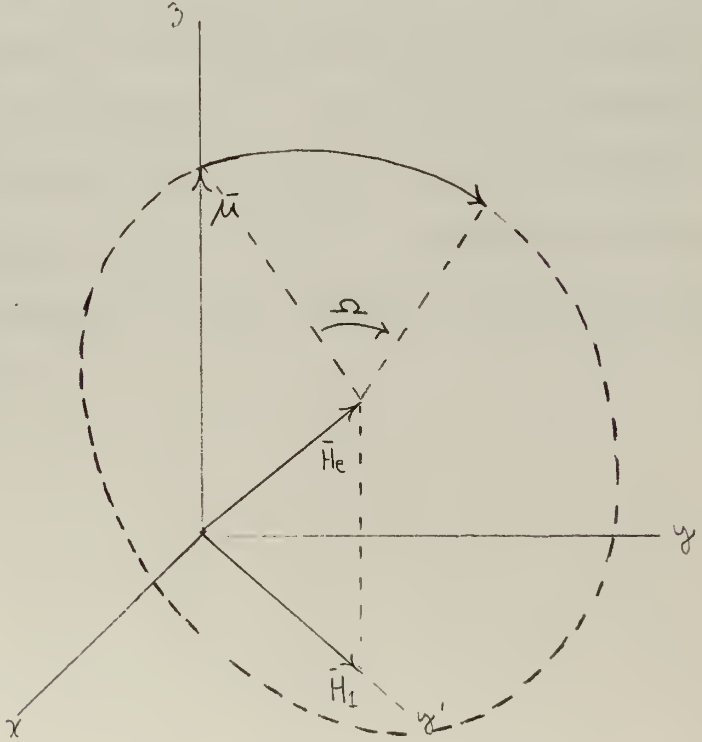

Fig. 2.10 Diagram of Magnetic Resonance

Now as the angular momentum is related to the magnetic moment by a constant, γ , such that $\bar{\mu} = \gamma \bar{M}$

$$\left(\frac{d\bar{M}}{dt}\right)^* = \bar{\mu} \times \bar{H}_0 - \bar{\omega} \times \frac{\bar{\mu}}{\gamma}$$
$$= \bar{\mu} \times \bar{H}_0 + \bar{\mu} \times \frac{\bar{\omega}}{\gamma}$$
$$= \bar{\mu} \times \left(\bar{H}_0 + \frac{\bar{\omega}}{\gamma}\right)$$

In particular, if $\bar{\omega} = -\gamma \bar{H}_0$ then $\left(\frac{d\bar{M}}{dt}\right)^* = 0$, and the effective field, $\bar{H}_e$, vanishes. The magnetic moment, $\bar{\mu}$, would see no torque in the rotating frame and would remain fixed with respect to it. The rotating frame is, therefore, simply riding along with the Larmor precession. Thus, $\bar{\omega} = -\gamma \bar{H}_0$ is shown to be the Larmor frequency.

How is this frequency related to the Zeeman split substates? These substates are separated by the energy of orientation of the $\bar{\mu}$ vector in the $\bar{H}_0$ field. From a classical viewpoint this energy can be expressed as $E = -\bar{\mu} \cdot \bar{H}_0$, but from the quantum viewpoint only discrete levels of this energy are allowed. Therefore, in this case, $E = -\gamma \frac{h}{2\pi} H_0 M$ where $M = -F, -F+1, \ldots F-1, F$. The energy level separation is seen to be $\Delta E = \gamma \frac{h}{2\pi} H$ and, converting ΔE to frequency, $\omega = \Delta E \frac{2\pi}{h} = \gamma H$. Thus the frequency corresponding to the energy level separation is seen to be the same as the Larmor frequency of precession.

D. Magnetic Resonance

It has already been shown that by postulating a coordinate system which rotates at the Larmor frequency about the z axis, the effective field, $\overline{H}_e$, can be reduced to zero. Now assume a coordinate system which is rotating at a frequency, ω, close to, but not necessarily at, the Larmor frequency. Further postulate an additional magnetic field, $\overline{H}_1$, which lies in the y-z plane at some angle, Θ, with the z axis such that $\tan\Theta = \frac{H_1}{H_0 - \omega/\gamma}$ (See Fig. 2.10). In this frame, an atomic magnetic moment will undergo a precession about $\overline{H}_e$ at a frequency, Ω, such that $H_e + \frac{\Omega}{\gamma} = 0$. If, for example, the magnetic moment is initially aligned with $\overline{H}_0$, the motion of the moment can be described. The effect of $\overline{H}_1$ is to reorient $\bar{\mu}$. Denoting the angle between $\bar{\mu}$ and $\overline{H}_0$ by α, it follows that $\cos\alpha = 1 - 2\sin^2\theta \sin^2\left(\frac{\Omega t}{2}\right)$ where $\Omega = \gamma\left[\left(H_0 - \frac{\omega}{\gamma}\right)^2 + H_1^2\right]^{1/2}$

It can be seen that, as $H_0 - \frac{\omega}{\gamma}$ approaches zero, appreciable tipping of the moment occurs. At resonance ($H_0 = \frac{\omega}{\gamma}$) the moment oscillates from +z to -z and back again at a rate $\Omega = \gamma H_1$ as $\overline{H}_1$ rotates about z at the Larmor frequency. This is the phenomenon of magnetic resonance.

z Axis Detection

Consider now a sample of rubidium vapor located at the center of coordinates. In addition to the ambient field, $\bar{H}_0$ along the z axis, there is an $\bar{H}_1$ field rotating in the x-y plane about the z axis. This field might be one of two components oppositely rotating in the x-y plane such that the total field could be described as

$$H_x = H_1 \cos \omega t$$

$$H_y = H_1 \sin \omega t$$

$$H_z = H_0.$$

If ω is made to approach the Larmor precession frequency, magnetic resonance occurs and reorientation of the $\bar{\mu}$ vector takes place. The effect is to make the population distribution of the M substates random. Because the substates are distributed almost randomly to start with, there is no observable effect.

Now, if circularly polarized D_1 light is caused to irradiate the sample along the z axis, optical pumping occurs. In equilibrium, the substates from which pumping is most likely are depleted, while the substates from which pumping is least likely are overpopulated. Thus the probability of a photon being lost from the pumping beam is reduced considerably compared to the probability of loss in the case of an unpumped sample.

When, however, the frequency of the oscillating $\bar{H}_1$ field, ω, is caused to approach the Larmor frequency the magnetic moments are reoriented and the population of pumped substates is redistributed

in a random manner. The transmitted light intensity is consequently reduced as more photons are lost from the beam.

This dip in light intensity can be detected with a photocell, as ω passes through resonance. By observing this effect on an oscilloscope, with the photocell output connected to the vertical deflection system and the frequency sweep (of $\overline{H}_1$) connected to the horizontal deflection system, a picture of the resonance line can be obtained.

Cross Beam Detection

A method of detection, which for some purposes is more useful, is the cross beam detection system.

Consider a second beam of D_1 light optically similar to the z beam but at right angles to it, say along the x axis. It is found that such a beam of light is intensity modulated at the frequency of the rotating $\bar{H}_1$ field when that frequency is equal to, or very close to, the Larmor frequency. The reasons for this light modulation will now be examined.

In an unpumped sample the expectation of the magnetization vector, denoted $\langle \bar{M} \rangle$, is zero or very close to zero. In a pumped sample, however, assuming no $\bar{H}_1$ field, the most probable position of the $\bar{M}$ vectors is in a cone about the z axis so that $\langle \bar{M} \rangle = M_z \bar{z}$. Now, if the $\bar{H}_1$ field is caused to rotate about the z axis, at or near the Larmor frequency, so that magnetic resonance occurs, $\langle \bar{M} \rangle$ will have a time varying component in the x-y plane. If this effect is examined from a coordinate system which rotates with $\bar{H}_1$ (let $\bar{H}_1$ lie along the new y axis, for example), it is seen that the $\bar{M}$ vectors precess about the $\bar{H}_e$ vector, which becomes the $\bar{H}_1$ vector at resonance; and thus, there occurs a net alignment along the x axis. This effect is complicated by relaxation action, which tends to disperse the alignment.

By use of a matrix treatment of the Bloch[1] equations of motion, Jaynes[2] obtains a solution for this alignment, as seen from

---

[1] F. Bloch, Phys. Rev., 70, 460, (1946)

[2] E. T. Jaynes, Phys. Rev., 98, 1099, (1955)

laboratory coordinate system. The equation, slightly modified to fit the optically pumped case, is:

$$M_y(t) = \frac{M_z^* \omega_1 T}{1 + b^2 T^2}\left(\cos\omega t - \Delta\omega T \sin\omega t\right) + \frac{M_z^* \omega_1 T}{b(1+b^2T^2)^{\frac{1}{2}}}\, e^{-t/T}\Big[\Delta\omega \sin(bt+\theta)\sin\omega t - \\ - b\cos(bt+\theta)\cos\omega t$$

Where M^*_z is the equilibrium pumped magnetization, $\omega_1 = \gamma H_1$, $\Delta\omega = \gamma H_0 - \omega$, $\tan\theta = bT$, $b = \left[(\gamma H_1)^2 + (\gamma H_0 - \omega)^2\right]^{\frac{1}{2}}$ and T is the relaxation period.

This equation reduces, in the case of steady state resonance, to:

$$M_y(t) = \frac{M_z^* \gamma H_1 T}{1 + \gamma H_1^2 T^2} \cos\omega t$$

Here it is seen that the $\overline{H}_1$ field has produced a net alignment in the x-y plane which rotates about the z axis. It is likewise observed that as $\overline{H}_1$ is increased from zero, M_y max builds up to a saturation level and then decreases.

Now it must be recalled that the second, or monitoring light beam, has its optical axis along the x axis, and thus the net angular momentum vector, which represents the spin systems, alternately points towards, and away from, the light source.

Consequently, the spin systems appear to the monitoring beam to possess a time varying angular momentum. When the angular momentum vector points toward the source, the angular momentum shall be defined as positive. Now since the photons in the monitoring beam can be absorbed by the spin systems only by delivering a change of angular momentum so that $\Delta M = +1$, it is seen, from the earlier mentioned pumping probabilities, that little light will be extracted from the

beam when the net momentum vector points toward the source. Conversely, when the net momentum vector points away from the source, maximum energy is extracted from the beam. Thus, the light is modulated at the Larmor precession frequency.

It has been assumed in the preceding discussion that the $\overline{H}_1$ field has been rotating in the positive direction with reference to $\overline{H}_0$, thus exciting the F=2 transitions. If the $\overline{H}_1$ field is caused to rotate in the opposite direction so as to excite the F=1 transitions, it must be remembered that the angular momentum vector is oppositely aligned with respect to the magnetic moment. Thus, with respect to the $\overline{H}_1$ field, the net momentum vector, and hence the light modulation, is 180° out of phase with the modulation produced in the case of the F=2 transitions. Also, the Larmor frequency is approximately 1500 cycles per second higher for the F=1 transitions. These differences make it possible to differentiate between the F=2 line and the F=1 line.

45 Degree Single Beam Detection

It is possible to obtain what is essentially cross beam detection by utilizing a single beam oriented 45° from the $\bar{H}_0$ axis. This beam acts both as a pumping beam and as a monitoring beam, for it may be resolved into two components, one parallel to the z axis and one parallel to the x axis. It would seem that, as each component is only about 70% as intense as in the cross beam case, the signal should suffer a considerable loss. Experiments, however, as performed by the writer, have not shown this to be the case. On the contrary, better signals seem to be obtained using the 45° beam system.

F. The Effect of Rotation

The effect of rotation upon the processes previously described will now be examined. Of chief interest is the effect of rotation of the entire experimental set-up with respect to some external coordinate system. Let the experimental coordinate system be at rest with respect to the external coordinate system. The frequencies of the F=2 line and the F=1 line are determined. Next, the experimental coordinate system is rotated about the $\overline{H}_0$ axis with a frequency, ω, positive with respect to $\overline{H}_0$. The atoms in the F=2 state are precessing in this same direction with a frequency, ω_2 referred to the external frame. This precessional frequency is determined only by the $\overline{H}_0$ field as determined in the external frame, and the rotation of the experimental frame has no effect upon the behavior of the precession as seen from the external frame. Therefore, as seen from the experimental frame, the precessional frequency is equal to $\omega_2 - \omega$, and if an observer in the experimental frame were to measure $\overline{H}_0$ solely by the precession of the F=2 state atoms, he would conclude that $\overline{H}_0$ had been reduced by an amount $\frac{\omega}{\gamma}$.

Now consider the effect upon the atoms in the F=1 state. Because these atoms are precessing in the opposite direction from the rotation of the experimental frame, an observer in this frame would determine that the frequency of precession had increased to $\omega_1 + \omega$. Guided solely by this evidence, he might conclude that $\overline{H}_0$ had increased by an amount $\frac{\omega}{\gamma}$. However, with both the F=1 line and the F=2 line to observe, it could only be concluded that the frame of reference was rotating at an angular velocity, ω.

Now if it is supposed that $\overline{H}_0$ changes at the same time that the experimental frame is rotated, it is found that both the rotation and the change in $\overline{H}_0$ can be detected unambiguously. Neglecting second order effects, and this may be done for rotations of less than 100 cycles per second, we obtain the following equations:

$$H_0 = \sqrt{\frac{\omega_1 \omega_2}{\gamma_1 \gamma_2}}$$

$$\omega = \omega_1 - \gamma_1 \sqrt{\frac{\omega_1 \omega_2}{\gamma_1 \gamma_2}}$$

where ω_1 and ω_2 are the observed frequencies of the F=1 and the F=2 lines, ω is the positive angular velocity of the experimental frame, and γ_1 and γ_2 are the ratios of the $\overline{H}_0$ field to the F=1 and F=2 frequencies, when the experimental frame is at rest.

It may be noted that the $\overline{H}_0$ field could be created artificially, inside the experimental frame. The spin systems need not have contact with the external frame through $\overline{H}_0$. For this reason, the rotation effect should be observed to occur within a completely closed system, such as in a space ship far distant from regions of appreciable magnetic fields.

III. The Equipment and the Experiments

The information to be obtained in the experimental work was primarily on the feasibility of detecting a rotation of the experimental frame by the method just described. The chief prerequisite was the ability to detect both the F=2 line and the F=1 line, and to be able to locate the line centers with reasonable accuracy. Because z axis detection cannot give information concerning the phase of the spin systems with respect to the $\overline{H}_1$ field, it was decided to use a cross beam system. The phase information thus gained can be used to locate the line centers with greater precision. The disadvantage of such a system is that the signal to noise ratio is not as good as it is with z axis detection. The first experiments were to determine whether or not the weak F=1 line could be observed at all.

A. The Components

The Lamp

The source of the rubidium light is a spherical pyrex bulb of about one milliliter volume containing a small amount of metallic rubidium and 1.5mm of argon as a filler gas. The bulb is located between the plate tank coils of a 100 Mcs oscillator, and the R. F. energy induces the discharge. The lamp emits the D_1 and D_2 lines of the rubidium spectrum. The intensity of these lines is dependent upon the temperature of the bulb which is best controlled by enclosing it in a small glass hood. The lamp assembly is enclosed in an aluminum shield, part of which is a parabolic reflector for collimating the light beam.

The Interference Filter

As has been previously described, only the D_1 light is desired. Thus the light beam is passed through an interference filter. This is a Spectralab filter which passes the 7948 Å D_1 line, and rejects the 7800 Å D_2 line.

The Circular Polarizer

In order to provide proper pumping action, as described, it is necessary that the light be circularly polarized. The circular polarizer consists of a linear polarizer followed by a quarter wave plate.

The Absorption Cell

The absorption cell is a pyrex cylinder, three inches long and two inches in diameter, containing a few milligrams of rubidium 87 and filled with a buffer gas. This buffer gas is argon at 3cm

pressure, the purpose of which is to reduce considerably the mean free path of the rubidium atoms. In this manner, the oriented rubidium atoms collide less often with the walls of the gas cell. Collisions with buffer gas atoms have a relatively small probability of causing loss of orientation compared to wall collisions. Thus, the addition of a buffer gas increases the relaxation time of the "pumped" rubidium atoms.

The Optics

The light coming from the lamp assembly is slightly divergent. It was discovered by experiment that the best pumping action was obtained by causing the light to converge slightly in the absorption cell. This was accomplished with a Fresnel lens of four inch diameter and three inch focal length. The lens was placed 2 1/4 inches in front of the cell. Another lens with the same characteristics was placed 2 1/4 inches beyond the cell to focus the transmitted light onto the photocell. Fig. 3.1 shows the position of the optical components.

The Photomosaic

The photosensitive material used to detect the modulation of the light beam was a Hoffman silicon solar battery. Because the capacitance of a single large solar cell is too high for the frequency used, nine small batteries were connected in series to form a photomosaic. This has an output resistance of 18K and an output capacitance of .002 μf .

The Preamplifier

The transistor preamplifier used was matched to the photomosaic

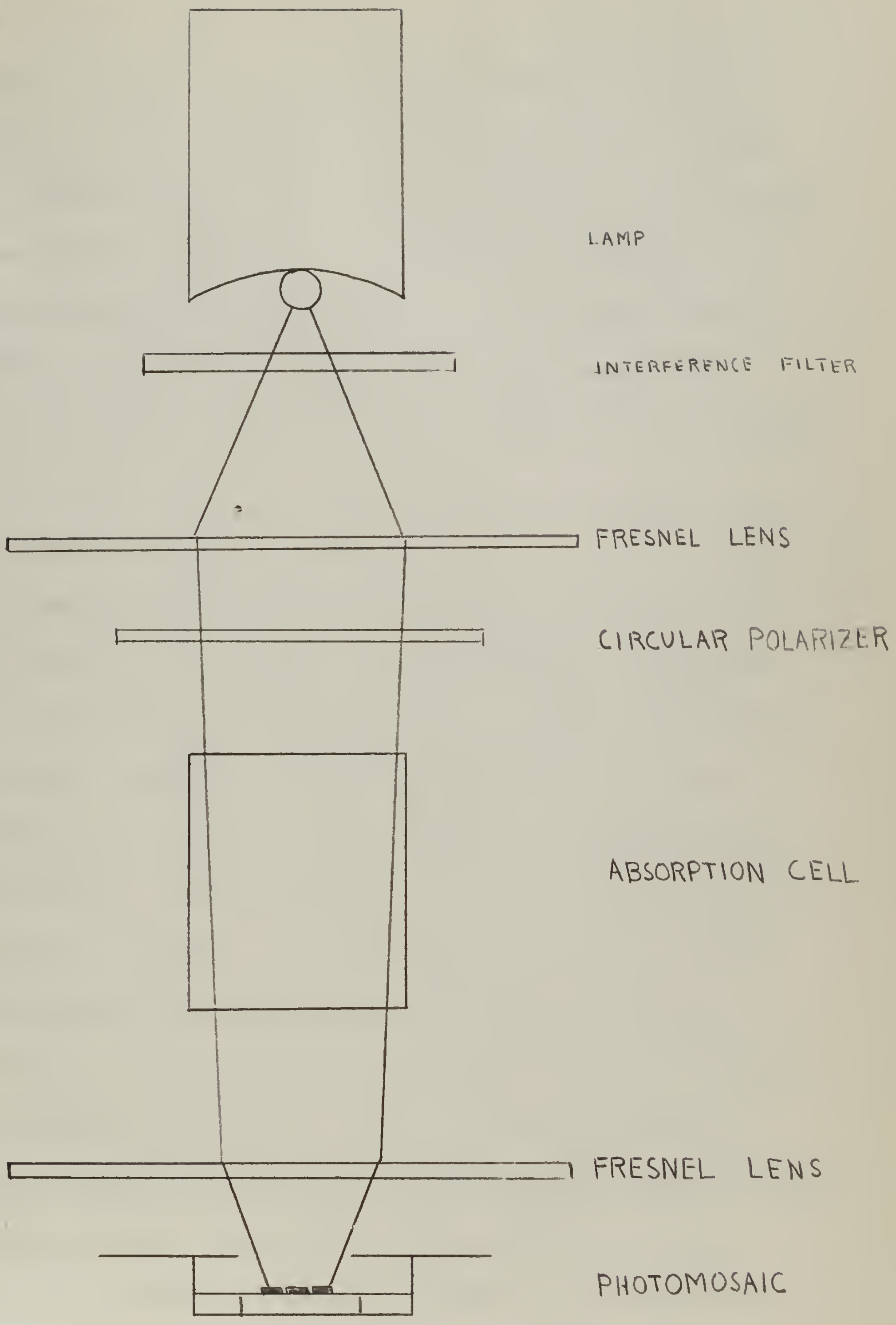

Fig 3.1 Diagram of Optics

and had a gain of approximately 150,000. The preamplifier was provided with two outputs. The first output was a low power, controlled phase shift output to be used in an oscillator feedback loop. The second output was of higher power and used for monitoring the signal. Because of the high gain of the preamplifier any ground loop was quite likely to cause unwanted oscillation. It was found that the R. F. shield about the photomosaic should be grounded to the input ground of the preamplifier, and that all other ground points should be connected to the ground at the output of the preamplifier. The circuit diagram is shown in Fig. 3.2.

The Mechanical Structure and Coil Systems

When the apparatus was set up for a cross beam experiment, the lenses, lamps, and cell were mounted on polyfoam blocks. The coils were mounted on the edges of a six inch cube of polyfoam that enclosed the absorption cell. When the 45° beam configuration was found to give a better signal to noise ratio, the mechanical arrangement was constructed as follows: A wooden platform was built with its top inclined 28° from the horizontal. A brass bearing was mounted on this top which was connected to a circular wooden platform 24 inches in diameter. The axis of rotation of this platform could thus be aligned with the earth's magnetic field, for the field at this location is inclined 28° from the vertical. On the rotating platform was mounted a cubical aluminum frame, 16 inches on an edge, which served to support the optical system at 45° from the earth's field and also as a coil form. The optical system was mounted in a cylindrical tube which was supported at diagonally opposite corners of the frame.

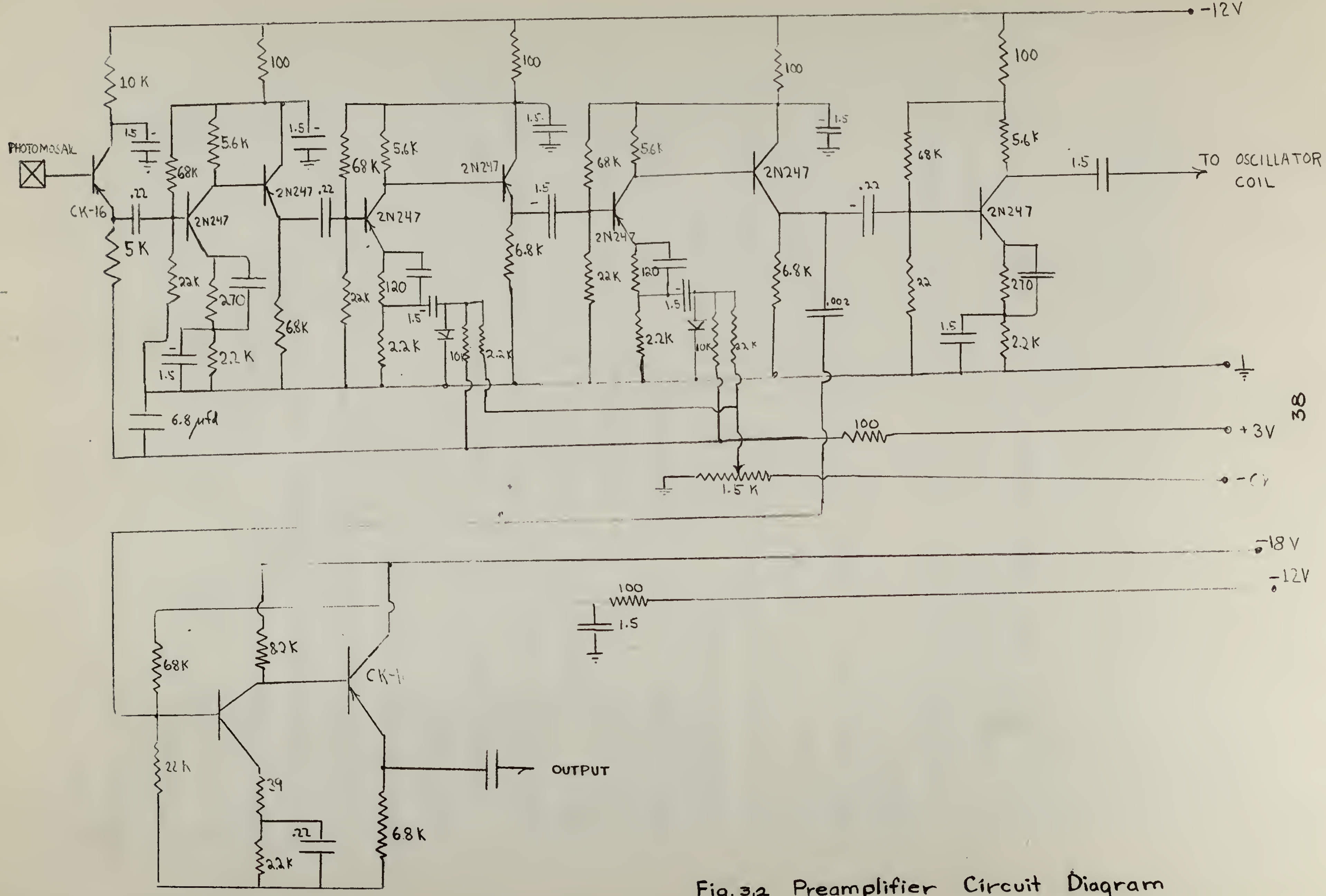

Fig. 3.2 Preamplifier Circuit Diagram

The coils, wound on the aluminum frame, consisted of two pairs of Helmholtz coils, the axes of which were perpendicular to the axis of rotation and to each other. Each coil was composed of approximately 12 turns of wire and adjusted so as to have 200 Ω reactance at 350Kc, as measured on a bridge. An additional smaller coil of 20 turns was wound about the absorption cell with a three inch diameter, and coaxial with the light beam. A photograph of the mechanical system is shown in Fig. 3.3.

Phase Shifter

The two pairs of Helmholtz coils were fed 90° out of phase with one another by a phase shift network. This network consisted of a 200 Ω resistance in series with one pair of coils and a 200 Ω resistor plus a 400 Ω capacitive reactance in series with the other pair of coils. The resistors and capacitors were adjustable for balancing. In this manner, the current through one pair of coils was made to lead the applied voltage by 45°, and the current through the other pair of coils was made to lag the applied voltage by 45°. A toggle switch was so connected that the pairs of coils could be interchanged.

The effect of the phase shifter was to circularly polarize the R. F. field in the vicinity of the absorption cell, the sense of circular polarization being determined by the toggle switch.

FIGURE 3.3 Photograph of Mechanical System

B. The Preliminary Experiments

The Detection of Resonance

The optics were aligned for a cross beam experiment. The pumping beam was set up along the $\overline{H}_0$ field, with the monitoring beam at right angles to the $\overline{H}_0$ field. With neither light nor $\overline{H}_1$ field, the noise output of the transitor preamplifier was examined on the Techtronics 310 oscillosoope. It was discovered that the noise was essentially gaussian in character. Next, an Allison 2-c tunable filter was inserted in the circuit between the preamplifier and the oscilloscope. The pass band of the filter was set for 350Kc. The noise was reduced considerably and was observed to have most of its energy concentrated between 300Kc and 400Kc. With the pumping light and monitoring light irradiating the absorption cell a slight increase in the noise level was observed. Now, the $\overline{H}_1$ field was applied with the phase shifter bypassed. With the frequency of the $\overline{H}_1$ field off resonance, only a very slight false signal, caused by direct R. F. pickup from the photocell resulted. If the horizontal sweep of the oscilloscope is synchronized to the $\overline{H}_1$ R. F. field, then this pickup remains stationary on the face of the scope as the R. F. frequency is slightly changed.

As the frequency is changed, however, another signal is seen on the scope which rapidly becomes larger as resonance is approached. When the $\overline{H}_1$ frequency is brought to within 100 cycles per second of resonance, the phase of the signal is observed to shift across the scope. This occurs because the phase of the atomic spin systems leads the exciting R. F. when the R. F. is at a frequency lower than resonance, and lags when the R. F. is at a frequency higher than

resonance. The position of zero phase lead can be considered the point of resonance.

It was found that when the amplitude of the exciting R. F. was high enough to produce noticeable pickup, the amplitude of the actual signal remained fairly constant over a range of several hundred cycles per second. This condition is one of R. F. saturation, and results in excessive line broadening. Should the R. F. be increased still further, the amplitude of the signal will actually decrease at the resonant point, resulting in a characteristic double "line". In order to observe a narrow line, the R. F. must be reduced considerably. Even with this precaution, the line width is about 150 cps. Now since the amplitude changes very little near the point of resonance where the phase changes most rapidly, it is clear that some method of phase detection would be more sensitive than would be a method employing amplitude detection.

Comparison of Cross Beam with 45° Beam Methods

It was discovered that the signal to noise ratio was a function of several variables. With the lens system optimized, it was found that the amount of current drawn by the lamp oscillators was important in achieving a good signal. The best signal was obtained with the oscillator power supplies set at 27ma. The temperature of the absorption cell was also very important. The signal to noise ratio obtained with the temperature at 35° C to 40° C, the best range, was about ten times the signal to noise ratio at 10° C.

The best obtainable signal to noise ratio, with the cross beam method, was approximately six to one. The pumping beam was now removed, and the apparatus tilted so that the axis of the monitoring beam was 45° from the $\overline{H}_0$ direction. A signal to noise ratio of approximately ten to one was achieved. All components were interchanged, where possible, to make certain that this improvement was not due to a faulty component in the pumping beam system. No significant difference was noted, and it became apparent that the 45° beam technique was superior to the cross beam method. This unanticipated result was further substantiated by repetitions of the experiment.

At this point the mechanical system, which was described earlier, was constructed and all further experiments were conducted with the 45° beam technique.

Detection of the F=1 Line

It now became important to detect the F=1 line. It had been assumed that the signal described previously was the result of

irradiating the F=2 transitions. An attempt was made to detect an additional effect at a frequency approximately 1500cps above the first signal. No such effect was noted. Considering the population probabilities, as previously outlined, it would be expected that the F=1 signal should be much weaker than the F=2 signal.

The next attempt to detect the F=1 signal utilized field rotation by means of the phase shifter. First, the $\overline{H}_1$ field was rotated at the Larmor frequency in the positive direction to detect the F=2 line and to obtain a reference. Then, the direction of rotation was reversed. It was observed that the F=2 signal disappeared. The frequency of the R. F. was then carefully raised until another signal appeared. This new signal was quite weak and disappeared when the direction of field rotation was again reversed. Next, the phase shifter was slightly misaligned so that the field was no longer circularly polarized, but eliptically polarized. Thus, when the field was caused to rotate in the negative direction a small positive component was also present. In this manner, both the F=2 and the F=1 lines could be seen, as the frequency was changed, at about equal strength. The frequency separation was approximately 1400 cps. The results of this experiment verify the prediction of the theory. It now remained to see if the F=1 and the F=2 lines could be used in a rotation detector.

Sequential Method of Line Separation Measurement

Now that both lines had been identified, it was decided to determine to what sensitivity the line centers could be located. It is easily seen that if one is to detect a rotation of one cycle

per second, the position of the F=1 line with respect to the F=2 line must be known to a precision of at least two cycles per second. In order to investigate the sensitivity to which the line centers could be located, the signal was put through an amplifier and then into a diode detector followed by a low pass filter. Thus, the signal amplitude was converted into a "D.C." level. Next, a coil was set up to provide a "hum" field coaxial to $\overline{H}_0$ with a frequency of 200cps. With this field established, the output of the detector was compared in phase with the 200 cps hum field. If, for example, the R. F. is at a frequency slightly lower than the line, the effect of the 200cps field will be to move the line into resonance when the hum field is instantaneously in opposition to $\overline{H}_0$. The comparison is accomplished with a phase comparator, the circuit of which is shown in Fig. 3.5. If the strength of the $\overline{H}_0$ field is slowly varied, the output of the phase comparator is essentially the derivative of the amplitude of the line. As the derivative changes most rapidly as it passes through zero at the center of the line, the method is rather sensitive.

The $\overline{H}_1$ field was rotated in the negative direction with a small positive component so that the F=1 line and the F=2 line would have roughly equal amplitudes. A helipot, driven by a timing motor, was set up to vary the $\overline{H}_0$ field so that with the proper $\overline{H}_1$ frequency both F=2 and F=1 lines could be swept through in a single "run". Thirty runs were made, fifteen of which produced useful data. This data was reduced to show the apparent variation in the frequency separation of the two lines. When the results were plotted, the variations in frequencies occurred in a roughly gaussian distribution

with a standard deviation of about 20cps. It is evident that it would be difficult to detect a one cycle per second rotation.

There are several possible causes of such variations between runs. It takes several minutes to sweep from the center of the F=2 line to the center of the F=1 line, and in this time the oscillator may drift. Also, the earth's field may change. If, due to lamp instability, the intensity of the light should change just as the center of the line is reached, this also may alter the apparent line center.

For these reasons it was seen to be desirable to somehow detect both lines simultaneously. A system using the F=2 line as a reference, and simultaneously comparing it to the F=1 line was thought to be a logical solution.

C. The Experimental System

It was decided from the results of the previous experiment that the two greatest sources of error were the changing magnetic field and the drifting of the oscillator. A method of overcoming both of these difficulties was devised by causing the system to oscillate on the F=2 line, and by using this oscillation as a reference frequency. Then, by mixing this frequency with 1420cps from a stable audio oscillator, a sideband at the F=1 frequency could be produced. Thus, a small additional modulation of the monitoring light beam would result which would have the effect of amplitude modulating the R. F. signal from the photomosaic. If this signal is detected, the 1420cps audio frequency can be recovered. If the F=1 line is precisely at the position of the upper side band, then the recovered audio will have the same phase as the audio from the oscillator. If, however, the F=1 line has been displaced upwards, due to a positive rotation rate about $\overline{H}_0$, the phase of the spin systems will lead the applied R. F. This phase lead will be preserved in the detection process and the recovered 1420cps will lead the applied 1420cps. Should the direction of the platform rotation be reversed it is seen that the recovered 1420cps will lag the applied audio. These phase changes can be observed with the phase comparator described previously.

The Additional Components

In order to complete the system as described, several additional components were needed. The first was a balanced modulator, to mix the F=2 signal with the reference 1420cps audio, to produce a sideband at the F=1 frequency. It was felt to be desirable to

suppress the F=2 frequency in the output. The circuit diagram of the modulator is shown in Fig. 3.6.

To drive the balanced modulator properly, the F=2 signal had to be amplified considerably. This was accomplished with a standard vacuum tube amplifier adjusted to provide an output of about 5V [illegible]

To produce a clean F=2 frequency, the Allison filter was replaced by a narrow band tuned amplifier, the circuit of which is shown in Fig. 3.7.

In order to produce the F=2 oscillation, the oscillator output of the transistor preamplifier was connected to the small 20 turn coil previously mentioned. When this coil was connected with the proper polarity, the system would self oscillate at the F=2 frequency

A standard aircraft radio receiver was used to detect the modulation in the signal at the output of the transistor preamplifier The antenna was loosely coupled to the input of the narrow band tuned amplifier, and the receiver tuned to the F=2 frequency.

Because of the large amount of extraneous noise in the output, an audio filter with relatively high Q was built and tuned to 1420cps. The circuit diagram of this filter is shown in Fig. 3.8.

The source of the 1420cps reference signal was a Hewlet Packard 200CD wide range oscillator with a balanced output. The output of the phase comparator was recorded on a Sanborn strip recorder.

The block diagram of the entire system is shown in Fig. 3.9.

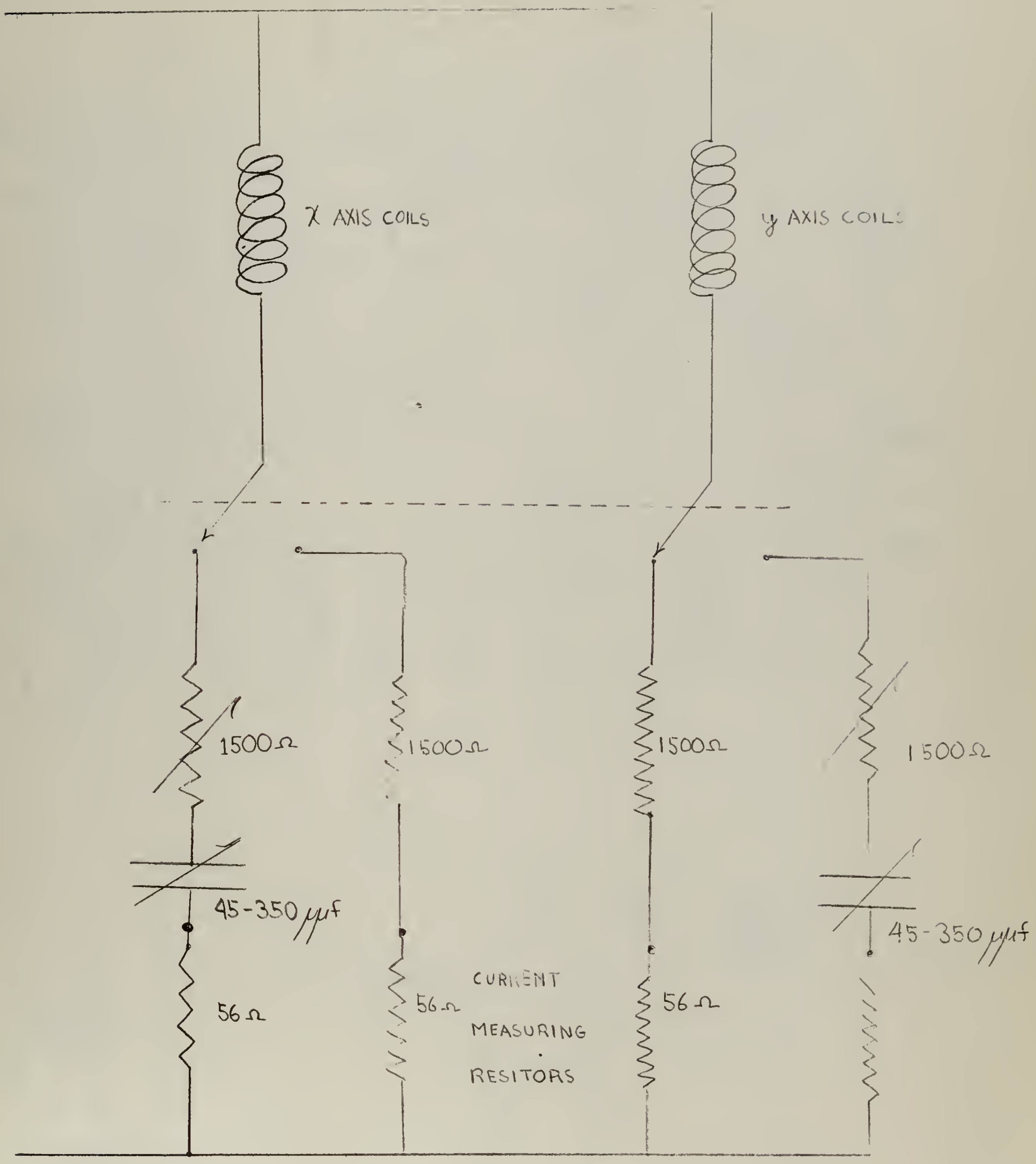

Fig. 3.4 Phase Shifter Circuit Diagram

Fig.3.5 Phase Comparator Circuit Diagram

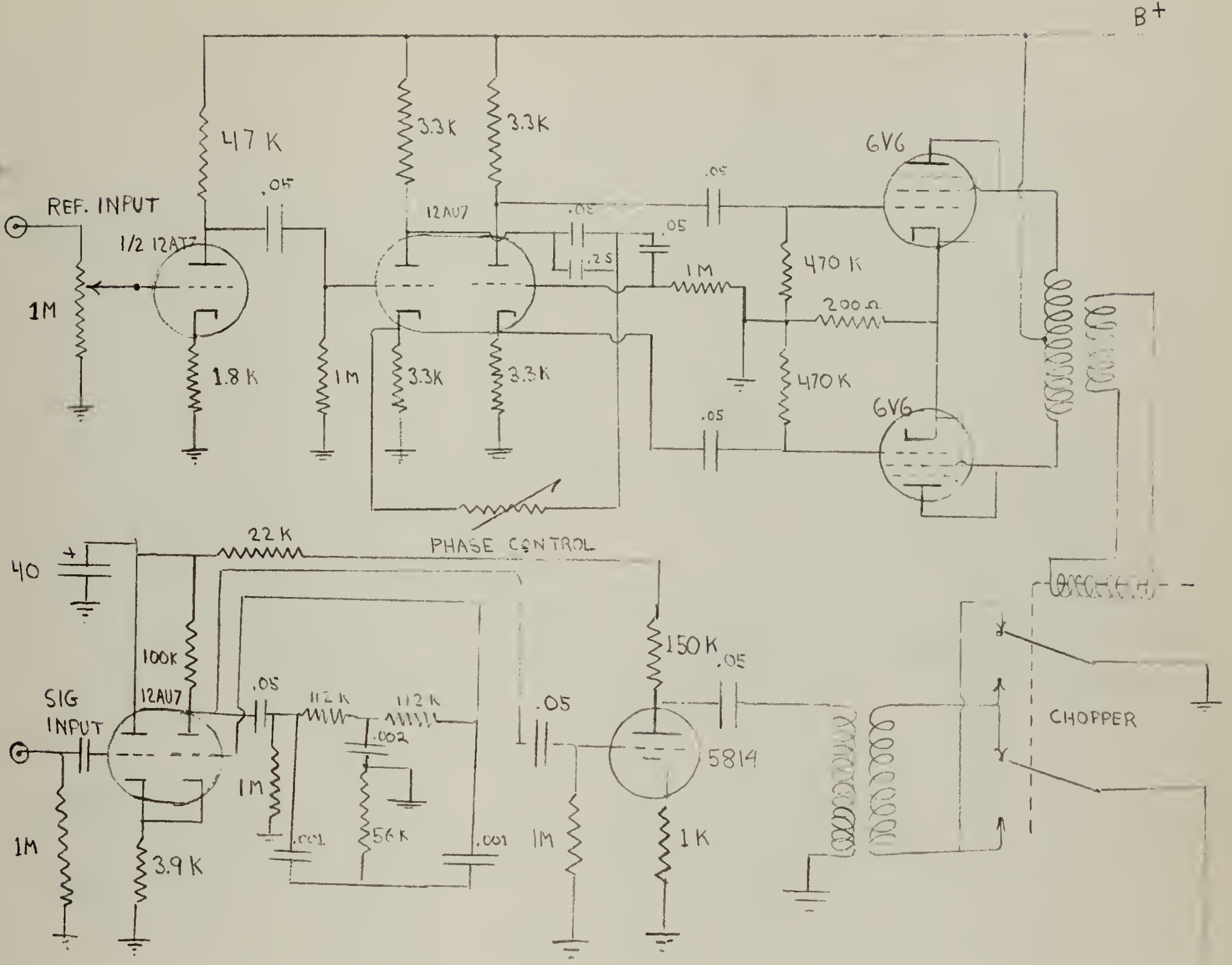

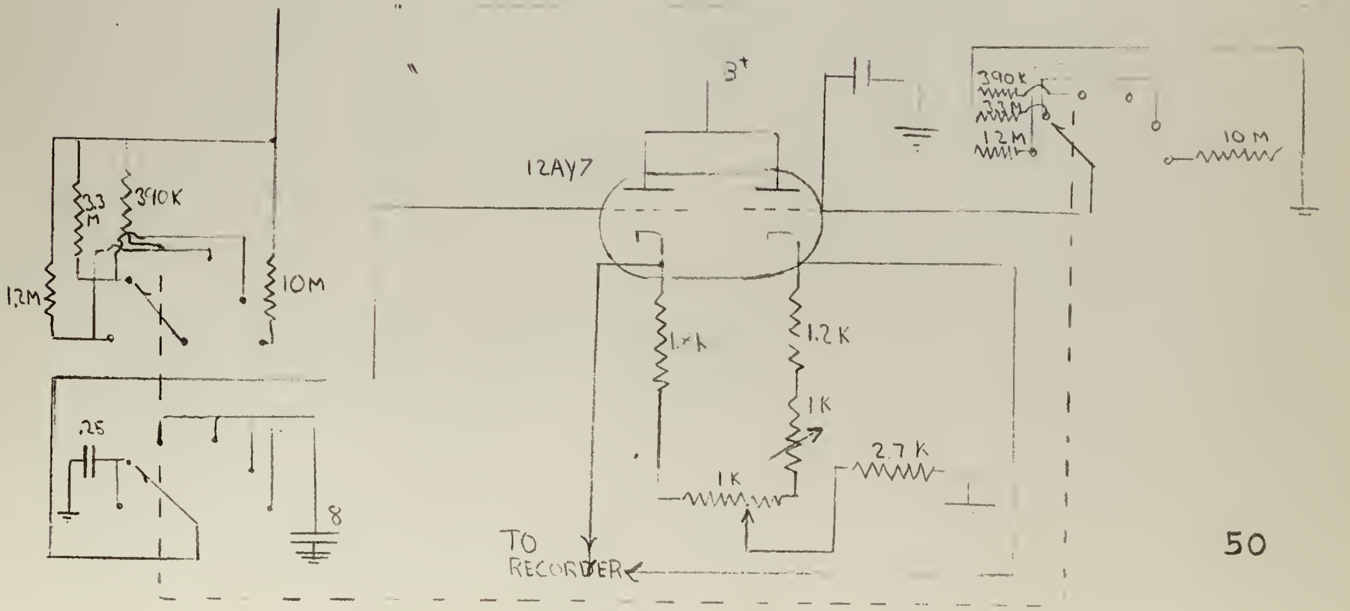

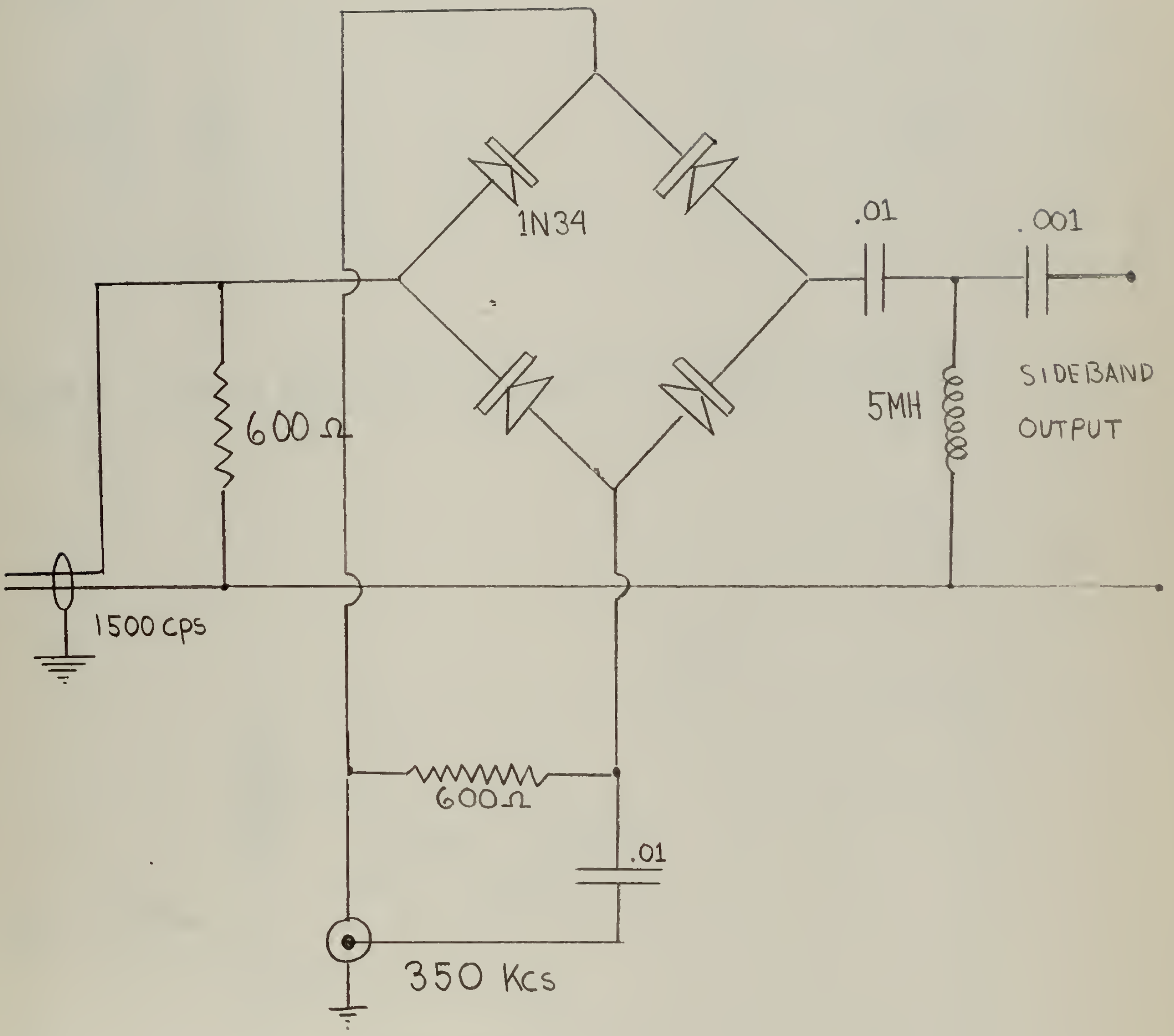

Fig. 3.6 Modulator Circuit Diagram

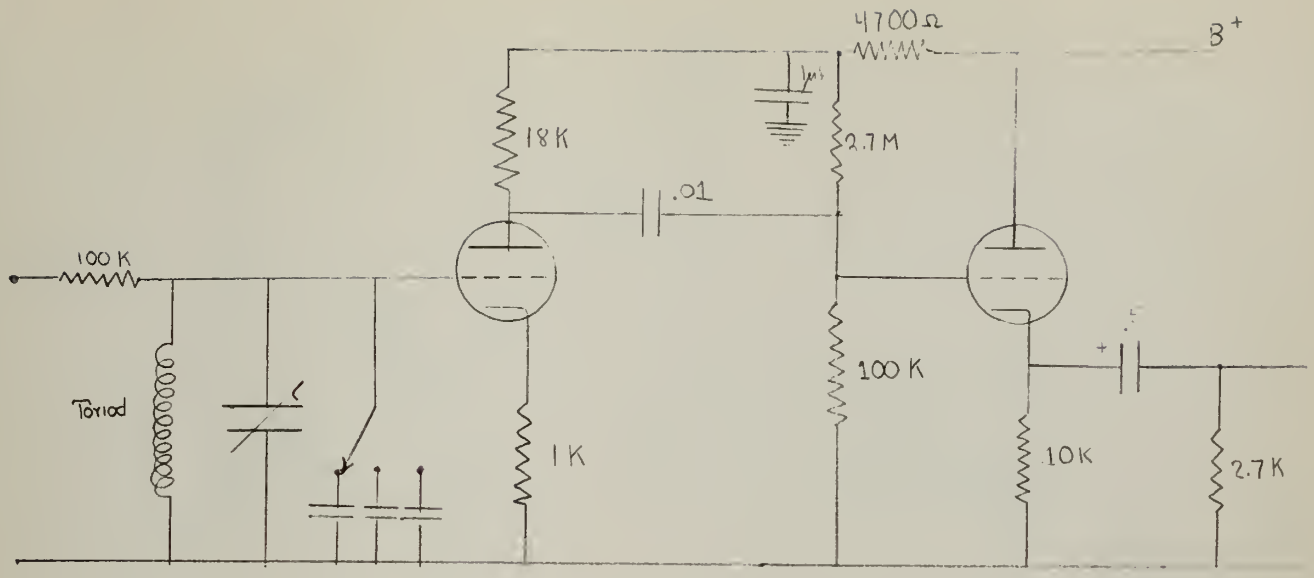

Fig. 3.7 Narrow Band Tuned Amplifier Circuit Diagram

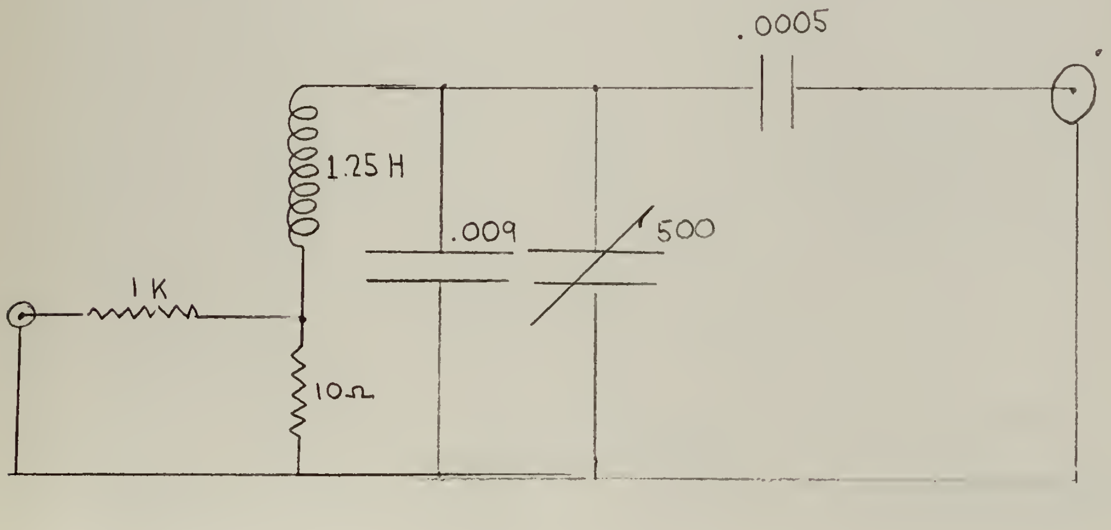

Fig. 3.8 Audio Filter Circuit Diagram

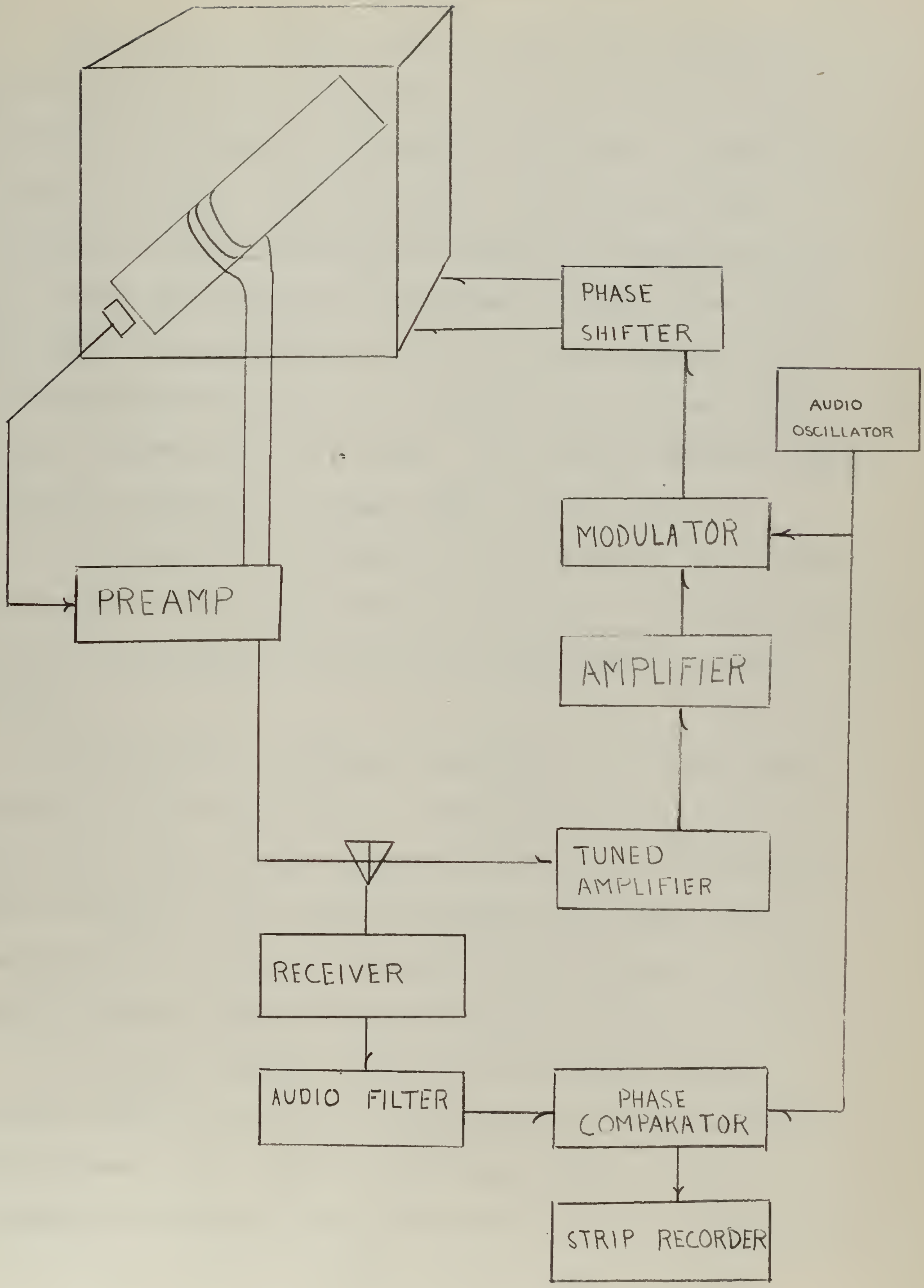

Fig 3.9 System Block Diagram

D. The Rotation Experiment

The system was activated with the output of the audio filter being examined on the oscilloscope. It was found that the noise impulses from the output of the radio receiver caused a considerable ringing in the audio filter at 1420cps. It was apparent that the amplitude of the F=2 oscillation was such that any amplitude modulation present was eliminated by saturation of the amplifier. As the absorption cell was allowed to cool below optimum temperature, and the amplitude of the oscillation decreased, the character of the signal from the audio filter changed. The variable amplitude ringing signal was replaced by a stronger steady 1420cps signal.

The sense of the polarization of the $\overline{H}_1$ field was then reversed so that the F=1 transitions would not be excited. The signal from the audio filter again became the same ringing type observed previously.

This experiment was performed repeatedly with the same results. It appears that the only possible explanation for such behavior is that the F=1 line is being irradiated, and that the F=1 transitions are modulating the light beam as described by the theory. No other explanation can account for the loss of audio signal when the sense of the circular polarization of the $\overline{H}_1$ field is reversed.

The output of the audio filter was then compared with the original 1420cps from the audio oscillator in the phase comparator. The frequency of the oscillator was adjusted until the phase comparator indicated zero phase difference. At this point, it would have been convenient to have had a filter of lower Q, for the

phase shift caused by detuning in the filter is easily confused with the phase shift caused by passing through the F=1 line. The latter effect, however, is somewhat sharper, and with a little care, may be distinguished from the phase shift due to the filter.

Once the line center was located, the output of the phase comparator was recorded on the Sanborn strip recorder. The output signal was observed with the platform at rest until its characteristics could be noted. The platform was then rotated. Because the platform could not be turned for more than one revolution in the same direction, and because (to obtain a reasonable signal to noise ratio) the integration, or smoothing time, on the phase comparator was set at .3 seconds, the maximum frequency of rotation that could be attempted was approximately one cycle per second. The platform was rotated and the resulting phase shift recorded on the Sanborn recorder. Fig. 3.10 shows some of the experiments made at different angular velocities. Although the effect of rotation is slight, it is plainly observable. Numerous attempts were made to produce similar effects by means other than rotation, such as lateral accelerations and tipping of the axis of rotation, but no such false rotation effects were noted.

Abscissa-one second per millimeter
Ordinate-relative phase shift, uncalibrated

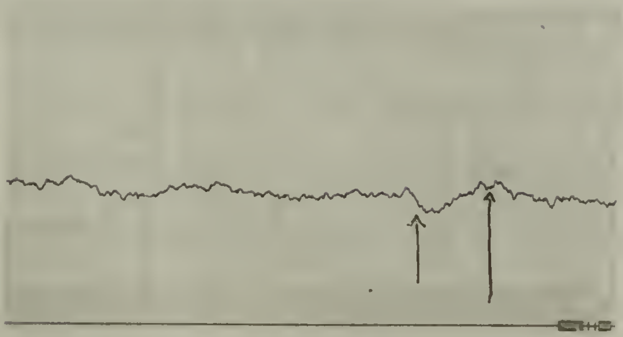

a) Negative rotation followed by positive rotation 2.5 radians displacement at rate of one radian per second

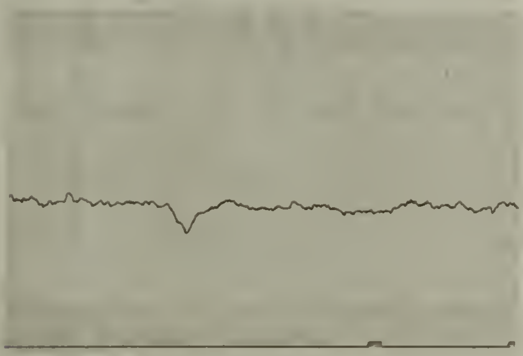

b) Negative rotation of two radians at 1.5 radians per second

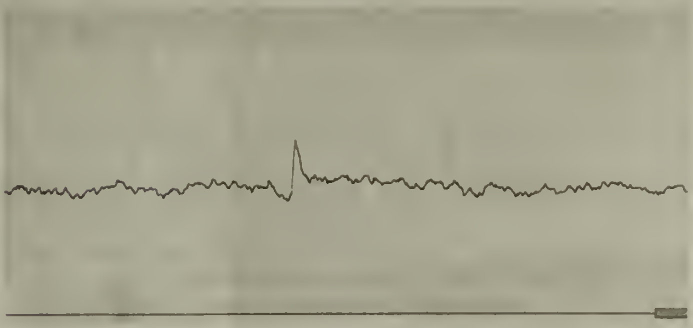

c) Positive rotation of 2.5 radians at three radians per second

FIGURE 3.10 Recording of Rotation Detection

IV. Evaluation and Conclusions

Summary of Results

By the method of circularly polarizing the $\overline{H}_1$ field, it has been demonstrated that the F=1 line and the F=2 line actually do represent the precessing rubidium atoms in their respective substates, and that the directions of precession are as predicted by theory.

It has also been demonstrated that the F=1 transitions can be induced simultaneously with the much stronger F=2 transitions. Even when the system is self oscillating on the F=2 line, it has been shown that the F=1 transitions, when induced, also modulate the monitoring beam, and that the two signals appear simultaneously at the output of the photomosaic. A system has been assembled which can detect a very small movement of these relatively broad lines.

Finally, it has been demonstrated that a rotation of the experimental frame can be detected by the shift of the F=1 and the F=2 lines as described by theory, and that a system can be assembled with the present state of the art which can measure this rotation.

Integration Time

Due to the relatively small angle through which the platform could be rotated, the length of time over which a measurement of rotation could be made was quite limited. For many applications, a much greater measurement time could be utilized. In this manner, the effects of the noise could be reduced greatly by integration methods, and a correspondingly smaller angular velocity measured.

The Need to Enhance the F=1 Transition

As has been emphasized earlier, the entire procedure is

made much more difficult because of the small F=1 signal. It is of prime importance in the further development of the system that some method be found to enhance the F=1 transition. The most logical approach is to attempt to redistribute the population probabilities by altering the method of optical pumping. This might be accomplished by changing the pumping light in some manner or by affecting the relaxation mechanism in the absorption cell.

V.

BIBLIOGRAPHY

1. Richtmeyer and Kennard, Introduction to Modern Physics, McGraw-Hill Co., 1947.

2. E. U. Condon and G. Shortley, The Theory of Atomic Spectra, Cambridge University Press, Cambridge, 1936.

3. H. G. Dehmelt, Phys. Rev., 105, 1487, 1957.

4. H. G. Dehmelt, Phys. Rev., 105, 1924, 1957.

5. W. B. Hawkins, Phys. Rev., 98, 478, 1955.

6. A. Kastler, J. Opt. Soc. AM., 47, 460, 1957.

7. G. E. Pake, Solid State Physics, Vol. 11, Academic Press Inc., Publishers, New York, N.Y., 1956.

8. W. E. Bell and A. L. Bloom, Phys. Rev., 107, 6, 1559-1565, 1957.

9. E. T. Jaynes, Phys. Rev., 98, 1099, 1955.